

F. Khaled\*, B. Allard, O. Ondel and C. Vollaïre

# Autonomous Flyback Converter for Energy Harvesting from Microbial Fuel Cells

DOI 10.1515/ehs-2015-0023

**Cover letter:** An autonomous flyback converter was designed for energy harvesting from Microbial Fuel Cells (MFCs). The circuit was optimized to minimize the losses and maximize the efficiency. A Maximum Power Point Tracking (MPPT) algorithm was implanted in the converter to extract the maximum power available from MFC. Discontinuous conduction mode operation of the flyback allows controlling the MPP operation by impedance matching. The flyback can start-up at low voltage, around 300 mV. The output open circuit voltage is about 20 V and the voltage at MPP is 6.4 V with a maximum efficiency of 71.2%.

**Abstract:** Microbial fuel cells (MFCs) use bacteria as the catalysts to oxidize organic matter and generate electricity. This energy can be used to supply low power electronic systems. A power management unit between the MFCs and the load is required to adapt the voltage and control the operation. The low voltage and low power characteristics of MFCs prohibit the use of standard converter topologies since the threshold voltage of standard CMOS transistors in CMOS technology is higher than the output voltage of MFCs. A low-voltage start-up sub-circuit is required to charge a primary capacitor to supply the driver. A specific sub-circuit is also required to control the operation of MFCs for Maximum Power Point Tracking (MPPT) issues. An optimized Discontinuous Conduction Mode (DCM) autonomous flyback converter for energy harvesting is presented for ambient sources, like MFCs. The converter is designed, fabricated, and tested. An MPPT algorithm is integrated in the system to control the operation and to extract the maximum available power from the MFC. The converter is able of start and step-up MFC output

voltage to a value higher than 3 V under load. The peak efficiency of the converter is 71.2%.

**Keywords:** converter, efficiency, maximum power point, microbial fuel cells, power, renewable energy

## 1 Introduction

Harvesting energy from ambient sources, through microbial fuel cell, Thermal Electric Generator (TEG) or mechanical vibrations, is a solution for replacing non-rechargeable batteries in low power electrical systems (Roundy et al. 2004). Many demonstrations of microbial fuel cells as viable power sources have been reported in literature to supply low-power electronics. Wireless remote sensors, for example, could be supplied from the electrical energy electrochemically converted from organic matter by means of MFC in a wastewater treatment plant (Dong et al. 2013; Tender et al. 2008; Donovan et al. 2011; Zhang, Tian, and He 2011). Developing micro-scale microbial fuel cells with a volume of 100s of  $\mu\text{L}$  makes them attractive to supply implantable medical devices and portable applications due to small size and lightweight (Ren, Lee, and Chae 2012; Ren et al. 2014). However the output voltage of these sources is limited below 1 V (Logan et al. 2006; Aelterman 2009). In order to produce sufficient voltage ( $>1.5$  V) to supply real applications, it is necessary to step-up the output voltage using a DC-DC converter that is able to start and operate at very low input voltage and to step-up voltage with a high ratio. To solve the start-up problem, an external power source was used in some converters to supply the oscillator at start-up (Wu et al. 2012). Many self-starting techniques were studied in literature. Mechanical switches or switched-based transformers were used to solve the start-up problem with low voltage sources (Ramadass 2011).

Many converter topologies have been studied for energy harvesting: flyback, boost, buck-boost (Grgic et al. 2009; Mateu, Pollak, and Spies 2007; Park 2012; Zhang et al. 2015). The flyback converter is the most interesting converter for low power applications due to its simpler control loop implementation, fast transient response and lower turn-on losses (Texas Instruments 2001). The main advantage is that the output voltage is isolated from the

\*Corresponding author: F. Khaled, Université de Lyon, INSA de Lyon, Ampère, CNRS UMR5005, 21 avenue Jean Capelle, 69100 Villeurbanne, France, E-mail: [firmas.khaled@insa-lyon.fr](mailto:firmas.khaled@insa-lyon.fr)

B. Allard, Université de Lyon, INSA de Lyon, Ampère, CNRS UMR5005, 21 avenue Jean Capelle, 69100 Villeurbanne, France

O. Ondel, Université de Lyon, Université Claude Bernard Lyon, 1, Ampère, CNRS UMR5005, 43 bd. du 11 novembre 1918, 69622 Villeurbanne Cedex, France

C. Vollaïre, Université de Lyon, école Centrale de Lyon, Ampère, CNRS UMR5005, 36 avenue Guy de Collongue, 69134 Écully, France

input by coupled inductors. This paper will include the circuit design, component selection and experimental tests of operation.

## 2 Electrical Characteristics

MFC has 0.7 L cylindrical reactor that is fabricated using commercially available low-cost PVC draining tubes. It is a single-chamber air cathode. Air-cathode is positioned at the edge for an equivalent cathode surface of 120 cm<sup>2</sup>. They are composed of 30% wet-proofed carbon cloth (Fuel Cell Earth) coated on the external side by 4 layers of PTFE and on the internal side by a catalyst layer with 0.5 mg.cm<sup>-2</sup> platinum and nafion as a binder. Layers are coated manually using a paintbrush. Electrical connections are realized by a titanium wire pressed against the cathode internal side. The anode is positioned in the middle. It is composed of electrically connected graphite fiber brushes (Gordon Brushes). Reactor was inoculated with wastewater from the effluent of the primary clarifier of a wastewater treatment plant. After start-up, the MFC was operated in fed-batch mode using 1 g/L of acetate as a fuel at room temperature.

The electrical characteristics of MFCs are presented as the polarization and output power curves. These characteristics were obtained by using a computer-controlled resistorstat changing load resistance and recording the voltage, the current and the power (Degrenne et al. 2012).

Figure 1(b) shows polarization and power curves of one MFC. The open circuit voltage is 580 mV. The maximum power is 755  $\mu$ W what means that the power density is about 1 mW/L (6.3  $\mu$ W/cm<sup>2</sup> of cathode surface). Higher values of open circuit voltage (0.6–0.9 V) and power densities (until 2.5 mW/L) were obtained. The organic fuel is generally consumed within an average of

25 days and the maximal allowable electric energy is in the range of 2 kJ/L /g of acetate which gives an energy conversion efficiency around 25%. The maximum power point occurs at 300 mV, i.e. 50% of the open circuit voltage. This property is to be used to control the maximum power by adapting the internal resistance of the converter to be equal to the internal resistance of the MFC (Jacobi's law).

## 3 Design of the Flyback Converter in DCM

### 3.1 Specifications

The converter design was based on the electrical characteristics of MFCs. The circuit should start and operate at low voltage about 0.3 V. The step-up ratio should be high to obtain sufficient output voltages. Because MFCs are strongly non-uniform generators, the converter should operate over a wide range of input power with a minimum power level of 300  $\mu$ W. Efficiency has to be maximized.

The flyback converter is divided into sub-circuits based on functions. This provides a straightforward way to design and analyse the circuit. The main sub-circuits of the flyback converter are the main circuit of the converter, start-up circuit, switching circuit, and the regulation as shown in Figure 2.

### 3.2 Start-up Circuit

The output voltage of the MFC is the principal input voltage of the start-up circuit. A minimum voltage of 1

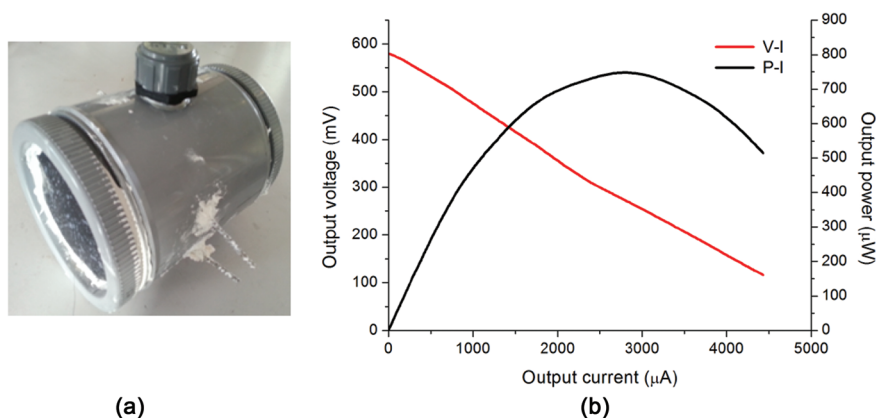


Figure 1: Photo of lab-scale MFC (a) and electrical characteristics of an MFC (b).

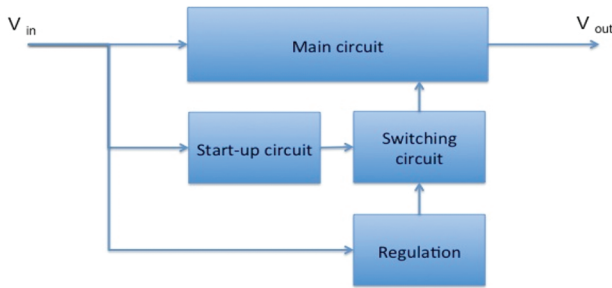


Figure 2: Main sub-circuits of the flyback converter.

$V$  is required to control the switching circuit in Figure 2. A step-up circuit is required for charging a primary capacitor. A commercial charge pump IC, S-882Z, is selected. The start-up voltage of the charge pump is about 300 mV what is compatible with the source specifications.

### 3.3 Switching Circuit and Regulation

The switching circuit is composed of an oscillator and a switch. The role of the oscillator is to drive the switch by producing a square control waves with controllable frequency and duty cycle. The choice of this controller has to be based on minimization of power consumption. The power consumption of the oscillator is usually a function of the supply voltage ( $V_{CC}$ ) and the frequency ( $f$ ). For example, at 25 kHz the supply currents are 1 and 7  $\mu\text{A}$  at supply voltages of 1 and 3 V which results in 1 and 21  $\mu\text{W}$ , respectively for the oscillator TS3001, from Touchstone Semiconductor. At 5 kHz, the power decreases to 0.7 and 14  $\mu\text{W}$  at supply voltages of 1 and 3 V, respectively. However the supply voltage and the frequency are not independent values since the output voltage of the oscillator drives the gate of the switch and

the frequency controls the internal impedance of the converter. The power consumption of the oscillator also depends on the power required for charge and discharge of the output capacitance ( $C_{OSS}$ ) of the switch. The power consumption of the oscillator TS3001 from Touchstone Semiconductor (1  $\mu\text{A}/1\text{ V}$ ), the low-level of supply voltage and the facility of control the frequency make it a very good candidate among the commercially available oscillators. One possible solution is possible to improve the performances of the converter is using the charge pump only at start-up. After start-up, there is an output voltage that can be used to supply the controller. The main advantage of this solution is to eliminate the charge pump after the start-up. The drawback is that the output voltage is not controlled and varies as function of the load. In an open circuit, for example, the output voltage is too high and it exceeds the nominal voltage of the controller. A solution was proposed in Wu et al. (2012) using diodes to adapt the output voltage to the nominal voltage of the controller. The power losses in the diode resistances and the required switching circuit are very important thus not acceptable in this design. If the output voltage is lower than the nominal voltage of controller, the output voltage will not be able to supply the controller. An additional circuit is required to regulate the oscillator supply voltage. The oscillator is therefore supplied from the output of the charge pump at all time of operation. The output frequency of the chosen oscillator can be controlled from 10 kHz to 110 kHz by modifying the resistance connected to the pin Rset, from 1 M $\Omega$  to 10 M $\Omega$  as shown in Figure 3(a). The frequency will be controlled by the input voltage ( $V_{in}$ ) as shown in Figure 3(b). Rset box represents a digital potentiometer architecture made of a resistor array controlled by MOSFETs ALD110902. Depending on the input voltage, the resistance Rset will be controlled to produce the desired

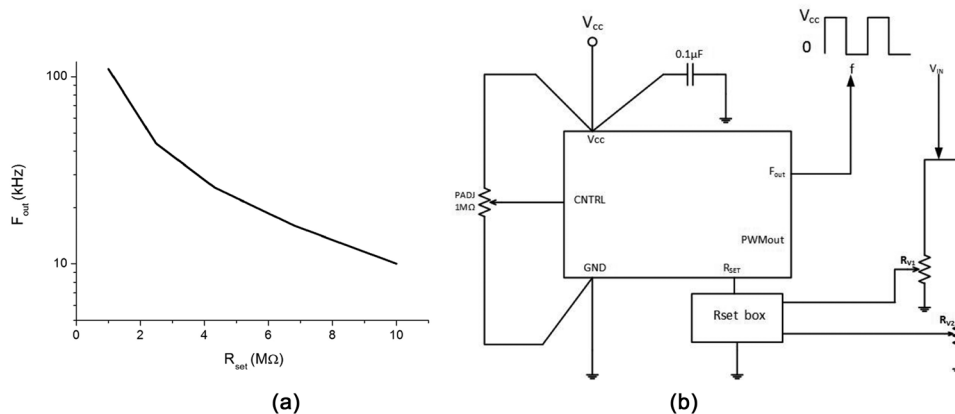


Figure 3: Characteristic of TS3001 oscillator (a) and circuit of TS3001 oscillator (b).

frequency. One modification on the input voltage will change  $R_{set}$  resistance by switching on or switching off one or more MOSFETs. That will create a new frequency value to modify the converter input resistance to extract the maximum power of the source.

### 3.4 The Main Circuit

The main circuit is a modified Flyback converter with two-coupled inductors. A discontinuous conduction mode (DCM) with a variable frequency is chosen to control the maximum power point (MPPT) adapting the internal resistance of the converter. DCM is usually the best choice for a low power flyback because it allows a smaller transformer and provides fast transient response and lower turn-on losses (Picard 2010). The flyback converter is detailed in Figure 4.

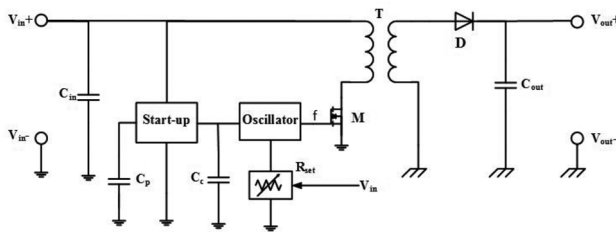


Figure 4: Circuit of the flyback converter.

#### 3.4.1 Selection of Switch

The gate of the switch is driven by the controller output voltage,  $V_{cc}$ . The threshold voltage of the switch has to be between 1 and 2 V. Moreover there are 2 types of losses in the switch: conduction losses and switching losses. Conduction losses are caused by the internal drain-source resistance of the switch,  $R_{DS(on)}$ , when it's crossed by the on-state current. Drain-source capacitance or the output capacitance ( $C_{oss}$ ) is present in all MOSFETs. During each cycle, the energy stored in  $C_{oss}$  is dissipated in the MOSFET, but the amount of energy dissipated can vary widely depending upon the MOSFET's structure. These losses are proportional to the switching frequency and the values of the parasitic capacitances. To minimize the total losses in the switch, the frequency  $f$ , the resistance  $R_{DS(on)}$ , the drain-source capacitance  $C_{oss}$  should all be minimized. The MOSFET FDV301N appears as a good candidate for the flyback converter. It has a low gate

Table 1: Specifications of MOSFET FDV301N.

Symbol	Description	Value	Unit
$R_{DS(on)}$	Static drain-source on-resistance at $V_{GS} = 2$ V	6.5	$\Omega$
$V_{GS(th)}$	Gate threshold voltage	1.06	V
$Q_g$	Total gate charge at $V_{GS} = 2$ V	200	pC
$C_g$	Grille capacitance	200	pF
$C_{oss}$	Output capacitance	10	pF
$t_{off}$	Turn – off fall time	3.5	ns

threshold voltage ( $V_{GS(th)} \approx 1$  V) and is suitable to be controlled by the selected oscillator, TS3001. It has an acceptable  $R_{DS(on)}$ , low turn-off time and low drain-source capacitance ( $C_{oss}$ ). Table 1 presents the main specifications of MOSFET FDV301N. The internal resistance of the flyback converter in DCM is independent of the input or output voltage and depends only on the primary inductance ( $L_{pri}$ ), the switching frequency ( $f$ ) and the duty cycle ( $d$ ), as given in eq. [1] (Adami 2013).

$$R_{in} = \frac{2 L_{pri} f}{d_m^2} \quad [1]$$

To ensure the operation in DCM over a wide range of input voltage and to simplify the control, the duty cycle was fixed to 0.5 (Paing et al. 2008). That also reduces the consumption of the control circuit because enabling the PWM function increases the TS3001's operating supply current from 5 to 10 times.

To determine the optimal switching frequency, the circuit was simulated using a model of MFC (Larminie 2003) consisting of a voltage source and a serial resistance for the minimum and maximum values of the internal resistances ( $R_{min}$  and  $R_{max}$ ). Experimental tests show that the internal resistance of the source varies between  $R_{min} = 100 \Omega$  and  $R_{max} = 200 \Omega$ . Taking into account eq. 1, the relation between the frequency and the primary inductor can be illustrated in Figure 5(a). Taking into account all losses produced by the main circuit and the control circuit, the maximum global efficiency was plotted against the switching frequency as shown in Figure 5(b). The simulated maximum global efficiency for low frequency is low because the switching speed is not enough to extract all the available energy. At high frequency, the losses in the circuit are more important. The efficiency therefore is low also. The optimal efficiency occurs around 10 kHz for the case of minimum resistance and 20 kHz for the case of maximum

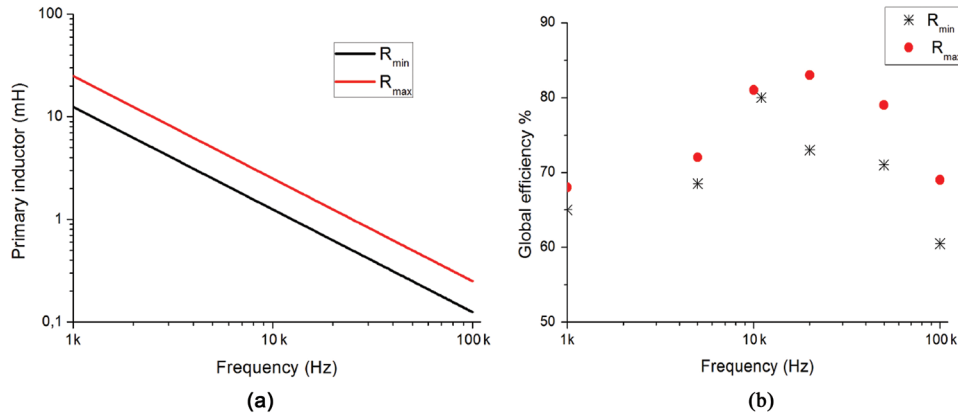


**Figure 5:** Primary inductor of flyback transformer vs the frequency (a) and global efficiency of flyback converter in function of switching frequency (b).

resistance. Moreover there is an inverse relationship between the size of a transformer and its frequency of operation. Taking for example a frequency of 1 kHz, the primary inductance is about 10 times larger than in the case of 10 kHz. The size of the transformer is approximately 3 times more than in the case of 10 kHz. On the other hand, the high frequency permits the use of a smaller transformer. However, losses increase at high frequency due to hysteresis and due to eddy currents circulating in the magnetic core of the transformer.

### 3.4.2 Design of Two Coupled Inductances

In a flyback converter designed to operate in a discontinuous mode, the required inductance value is less and the inductor physical size may be smaller than a flyback converter designed to operate in a continuous mode. That is because the output voltage in a DCM flyback converter is independent of the turn ratio  $m$ . In order to minimize the size of the transformer and the secondary resistance, the turn ratio can be taken as  $m = 1$ . As discussed before, the optimal efficiency occurs around a frequency of 10 kHz and 20 kHz for the case of  $R_{min}$  and  $R_{max}$  respectively. From Figure 5(a), the corresponding value of the primary inductance is  $L_{pri} = 1.25$  mH. The number of turns can be calculated using the inductance factor ( $A_L$ ) defined in eq. [2]. It is a manufacturing constant expressed in nH/turn<sup>2</sup> or as abbreviation in some data-sheets in nH.

$$A_L = \frac{L}{N^2} \quad [2]$$

The selected core is a ferrite ring toroid core that has the following characteristics:  $A_L = 2,775$  nH, Internal diameter 7.9 mm, External diameter 12.7 mm.

From eq. [2] and the inductance factor of the core, the number of turns of primary inductor,  $N_{pri}$ , can be

calculated and is equal to 21 turns. Considering  $m = 1$ , the number of turns of the secondary inductor,  $N_{sec}$ , is equal to 21 turns. The primary and secondary turns are fabricated with 0.56 mm<sup>2</sup> copper wire to minimize the ohmic resistance of the transformer.

### 3.4.3 The Diode

The diode allows the current at defined voltage to flow from the secondary inductor to be stored in the capacitor. It also prevents the current flow in the reverse direction. In a DCM, there is no diode reverse recovery loss. The low level of voltage requires a diode with a low threshold voltage, low  $R_{DS(on)}$  and low diode capacitance to limit the conduction and commutation losses. Many diodes were tested for this circuit. Two of them, BAT54 and HSMS-282, have almost the same performances. A Schottky diode BAT54 was selected because it presents the lowest losses. Specifications of BAT54 are: forward voltage (240 mV), on-resistance (2  $\Omega$ ) and junction capacitance (10 pF).

## 4 Results and Discussion

The circuit is primarily fabricated on a printed circuit board (PCB) using discrete off-the-shelf components (Figure 6). The layouts are designed to try and minimize the overall size. To minimize size, components are placed on both sides of the board.

### 4.1 Test of the Flyback Converter with a Model of the Microbial Fuel Cell

The converter was tested with a simple model of microbial fuel cell in open circuit voltage and for a load of



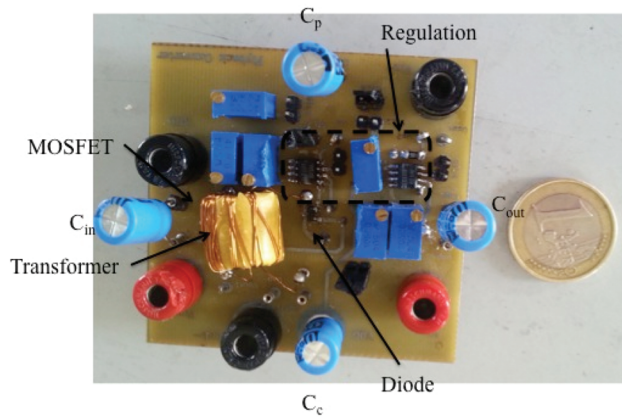


Figure 6: Printed circuit board of the prototype.

50 k $\Omega$ . The simple model of MFC, as any power source, consists of a voltage source equal to the open circuit voltage of the MFC (580 mV) serially connected with a resistance equal to the internal resistance of the MFCs (106  $\Omega$ ). The maximum power delivered by this model is 793  $\mu$ W. Figure 7 presents the control frequency (blue), the output voltage (cyan), the voltage across the capacitor  $C_c$  (magenta) and the voltage across the capacitor

$C_p$  (green) in open circuit and over a load of 50 k $\Omega$ . This figure presents the start-up of the converter. Since the input voltage is higher than the start-up voltage of the charge pump, it starts-up and the voltage of the capacitor  $C_p$  raises. When it becomes 2.4 V, the capacitor  $C_p$  starts to discharge into the capacitor  $C_c$ . When the voltage of  $C_c$  arrives to 1 V, the oscillator starts to drive the MOSFET and the output voltage starts to rise. The output voltage in open circuit is 19.5 V. The converter is tested also for a load of 50 k $\Omega$ . The output voltage was 5.3 V. The efficiency calculated as the relation between the output power and the maximum power to be delivered is 70.8%. The efficiency calculated as the relation between the output power and the input power is 73.3%. The extracted power therefore is equal to 96.5% of the maximum power that could be delivered. The curve of the efficiency as a function of the load was plotted in Figure 8(a). The output voltage is tested as a function of the input voltage for two loads: 1 M $\Omega$  and 10 k $\Omega$  in Figure 8(b). The start-up voltage of the converter is about 320 mV. This voltage is limited by the start-up voltage of the charge pump. Using an external source to supply the controller, the start-up voltage decreases to 135 mV.

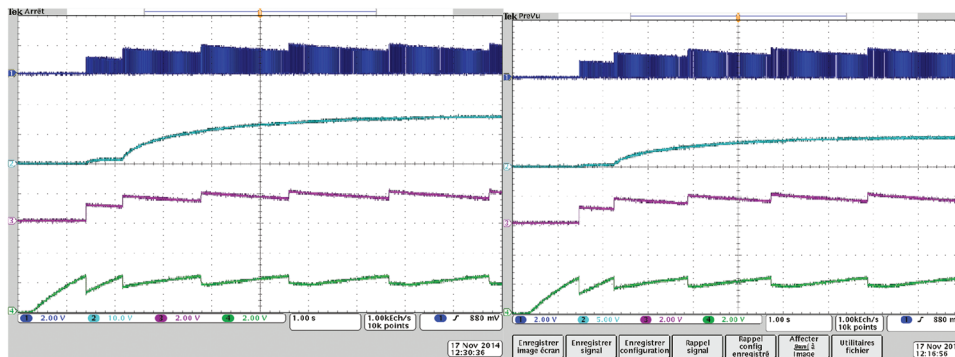


Figure 7: Shows the control frequency (blue), the output voltage (cyan), the voltage across  $C_c$  capacitor (magenta) and the voltage across  $C_p$  capacitor (green) in open circuit (left) and over a load of 50 k $\Omega$  (right).

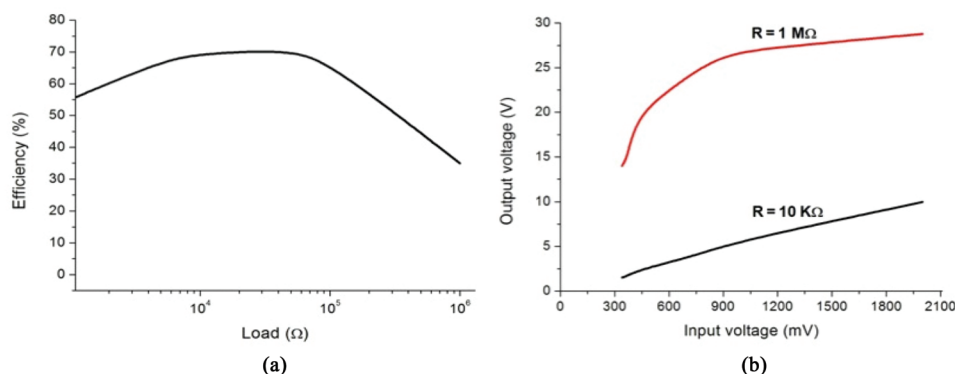


Figure 8: Efficiency of flyback converter as a function of the load (left) and Output voltage as a function of the input voltage for two loads 1 M $\Omega$  and 10 k $\Omega$  (right).

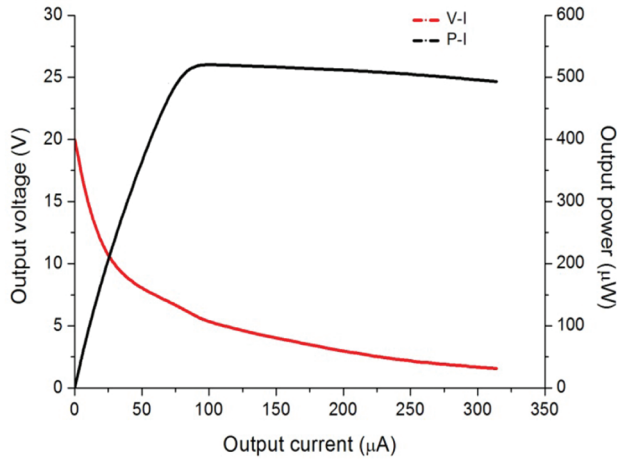


Figure 9: Output voltage and output power of the flyback converter supplied by the MFC as a function of the current.

## 4.2 Test of the Flyback Converter with a Real Microbial Fuel Cell

The converter was also tested with a real microbial fuel cell. The static characteristics of the MFC are presented in Figure 1. The MFC was able to start-up the converter and the operation was the same as the one presented in Figure 7. The output voltage and the output power were plotted as functions of the output current in Figure 9. The open circuit voltage is about 20 V and the voltage at MPP is 6.4 V for a load of 76 kΩ. The maximum output power is 538 μW. The maximum efficiency is 71.2%. The frequency was measured and equals to 10.5 kHz.

## 4.3 Losses' Analysis

Losses in the flyback converter are evaluated analytically. Table 2 shows the breakdown of these losses. There are three types of losses in the MOSFET. The conduction

Table 2: Losses in flyback converter.

Losses	Description	Value
<b>MOSFET</b>		
$P_{cnd\_Mos}$	Conduction	128 μW
$P_{sw\_toff}$	Switching triangle	1.28 μW
$P_{sw\_Coss}$	Sw. Output Cap.	2.23 μW
<b>Diode</b>		
$P_{cnd\_d}$	Conduction	24.7 μW
$P_{sw\_Cj}$	Junction Cap.	0.15 μW
<b>Inductances</b>		
$P_{cnd\_ind}$	Conduction	23 μW
<b>Control</b>		
$P_{Driv}$	Driver	6 μW
$P_{ctrl}$	Controller	2 μW
$P_{reg}$	Regulation	2.5 μW
<b>Start-up circuit</b>		
$P_{start}$	Start-up circuit	30.1 μW
Total losses		219.96 μW

losses are presented by the ohmic resistance of the drain-source of the MOSFET, switching losses dissipated by charging and discharging the capacitor  $C_{oss}$  and cross-over losses what occur during the turn-off of MOSFET. The diode at the output of the flyback presents also conduction and switching losses. The resistances of primary and secondary coils of flyback transformer dissipate power. In the control circuit, the losses are the sum of the power consumption of the control circuit presented by the average consumed current when the controller is unloaded and the losses in the gate of MOSFET presented by the input capacitor. The power losses can be calculated as the product of the input voltage by the average start-up current ( $i_{start,avg}$ ) when the charge pump is unloaded. Figure 10 represents the distribution of these losses in the flyback converter. The most important losses occur in the MOSFET switch by conduction, 128 μW, although a low  $R_{DS(on)}$ . The total losses in the circuit were about 220 μW.

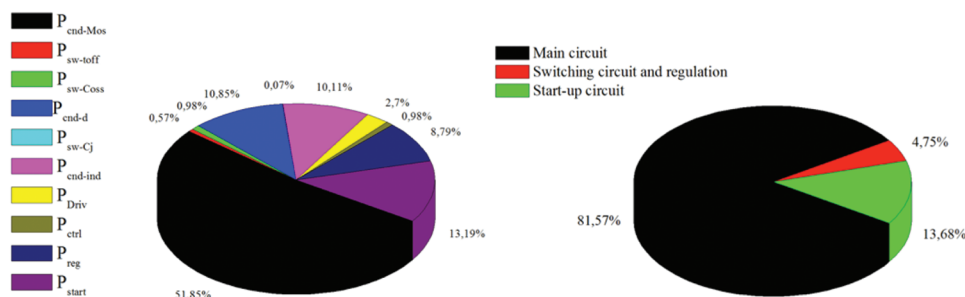


Figure 10: Losses in the flyback converter.

## References

- Adami, S. 2013. "Optimisation de la récupération d'énergie dans les applications de rectenna", thesis, école central de Lyon.
- Aelterman, P. 2009. "Microbial fuel cells for the treatment of waste streams with energy recovery". PhD thesis, Ghent University.
- Degrenne, N., F. Buret, B. Allard, and P. Bevilacqua. 2012. "Electrical Energy Generation From a Large Number of Microbial Fuel Cells Operating at Maximum Power Point Electrical Load." *Journal of Power Sources* 205:188–93.
- Dong, K., B. Jia, C. Yu, W. Dong, F. Du, and H. Liu. 2013. "Microbial Fuel Cell as Power Supply for Implantable Medical Devices: A Novel Configuration Design for Simulating Colonic Environment." *Biosensors and Bioelectronics* 41:916–19.
- Donovan, C., A. Dewan, H. Peng, D. Heo, and H. Beyenal. 2011. "Power Management System for a 2.5 W remote Sensor Powered by a Sediment Microbial Fuel Cell." *Journal of Power Sources* 196:1171–7.
- Grgić, D., T. Ungan, M. Kostić, and L. M. Reindl. 2009. Ultra-low input voltage DC-DC converter for micro energy harvesting. In *Proceedings of Power MeMs*, pages 265–268.
- Larminie, J., and A. Dicks. 2003. *Fuel Cell Systems Explained*, 2nd ed. Chichester: Wiley.
- Logan, B. E., B. Hamelers, R. Rozendal, U. Schröder, J. Keller, S. Freguía, and K. Rabaey. 2006. "Microbial Fuel Cells: Methodology and Technology." *Environmental Science and Technology* 40 (17):5181–92.
- Mateu, L., M. Pollak, and P. Spies. 2007. Step-up converters for human body energy harvesting thermogenerators. Technical Digest Power MEMS, pages 213–216.
- Paing, T., J. Shin, R. Zane, and Z. Popovic. 2008. "Resistor Emulation Approach to Low-Power RF Energy Harvesting." *IEEE Transactions on Power Electronics* 23 (3):1494–501.
- Park, J. D., and Z. Ren. 2012. "High Efficiency Energy Harvesting From Microbial Fuel Cells Using a Synchronous Boost Converter." *Journal of Power Sources* 208:322–7.
- Picard, J. 2010. Under the hood of flyback smps designs. TI Power Supply Design Seminar SEM1900.
- Ramadass, Y. K., and A. P. Chandrakasan. 2011. "A Battery-Less Thermoelectric Energy Harvesting Interface Circuit with 35 mV Startup Voltage." *IEEE Journal of Solid-State Circuits* 46 (1):333–41.
- Ren, H., H. Lee, and J. Chae. 2012. "Miniaturizing Microbial Fuel Cells for Potential Portable Power Sources: Promises and Challenges." *Microfluid Nanofluidics* 13 (3): 353–81.
- Ren, H., C. Torres, P. Parameswaran, B. Rittmann, and J. Chae. 2014. "Improved Current and Power Density with a Micro-Scale Microbial Fuel Cell Due To a Small Characteristic Length." *Biosensors and Bioelectronics* 61: 587–92.
- Roundy, S., D. Steingart, L. Frechette, P. Wright, and J. Rabaey. 2004. "Power Sources for Wireless Sensor Networks." *Lecture Notes in Computer Science* 2920:1–17.
- Tender, L. M., S. A. Gray, E. Groveman, D. A. Lowy, P. Kauffman, J. Melhado, R. C. Tyce, D. Flynn, R. Petrecca, and J. Dobarro. 2008. "The First Demonstration of a Microbial Fuel Cell as a Viable Power Supply: Powering a Meteorological Buoy." *Journal of Power Sources* 179:571–5.
- Texas Instruments. 2001. Inductor and flyback. Technical report, Texas Instruments.
- Wu, K., C. Biffinger, A. Fitzgerald, and R. Ringeisen. 2012. "A Low Power DC/DC Booster Circuit Designed for Microbial Fuel Cells." *Process Biochemistry* 47 (11):1620–6.
- Zhang, X., H. Ren, S. Pyo, J. I. Lee, J. Kim, and J. Chae. 2015. "A High Efficiency Dc-Dc Boost Converter for a Miniaturized Microbial Fuel Cell." *IEEE Transactions on Power Electronics* 30 (4): 2041–9.
- Zhang, F., L. Tian, and Z. He. 2011. "Powering a Wireless Temperature Sensor Using Sediment Microbial Fuel Cells with Vertical Arrangement of Electrodes." *Journal of Power Sources* 196:9568–73.